AD-A120 316 POLYTECHNIC INST OF NEW YORK BROOKLYN F/G 11/6
THE PROPAGATION OF SLIP ACROSS ALPHA/BETA INTERFACES IN TITANIU--ETC(U)
DEC 81 C HAMMOND, H MARGOLIN N00014-75-C-0793
UNCLASSIFIED NL

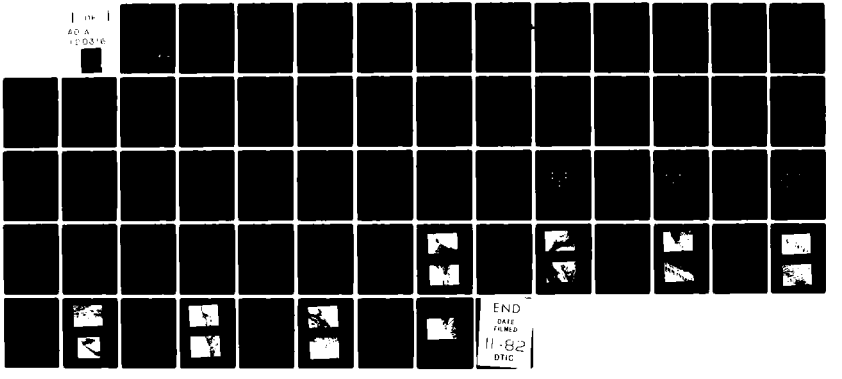

END
DATE FILMED
11-82
DTIC

THE PROPAGATION OF SLIP ACROSS α/β INTERFACES IN TITANIUM ALLOYS

by

CHRISTOPHER HAMMOND AND HAROLD MARGOLIN

Polytechnic Institute of New York
Brooklyn, N.Y.

December, 1981

Joint Report on AFOSR Grant # 79-0028 and
ONR Contract # N-0014-75-C-0793

To

Office of Naval Research and
Air Force Office of Scientific Research

SECURITY CLASSIFICATION OF THIS PAGE (When Data Entered)

REPORT DOCUMENTATION PAGE	READ INSTRUCTIONS BEFORE COMPLETING FORM
1. REPORT NUMBER: Joint AFOSR-ONR Report — 2. GOVT ACCESSION NO.: AD-A120 316	3. RECIPIENT'S CATALOG NUMBER
4. TITLE (and Subtitle)	5. TYPE OF REPORT & PERIOD COVERED: Interim Report
	6. PERFORMING ORG. REPORT NUMBER
7. AUTHOR(s): Christopher Hammond, Harold Margolin	8. CONTRACT OR GRANT NUMBER(s): AFOSR Grant #79-0028 and ONR #N-0014-75-C-0793
9. PERFORMING ORGANIZATION NAME AND ADDRESS: Polytechnic Institute of New York, 333 Jay Street, Brooklyn, NY 11201	10. PROGRAM ELEMENT, PROJECT, TASK AREA & WORK UNIT NUMBERS
11. CONTROLLING OFFICE NAME AND ADDRESS: Air Force Office of Scientific Research, Bolling Air Force Base, Washington, DC; Office of Naval Research, Arlington, VA	12. REPORT DATE: December, 1981
	13. NUMBER OF PAGES
14. MONITORING AGENCY NAME & ADDRESS (if different from Controlling Office)	15. SECURITY CLASS. (of this report)
	15a. DECLASSIFICATION/DOWNGRADING SCHEDULE

16. DISTRIBUTION STATEMENT (of this Report)

Distribution Unlimited

17. DISTRIBUTION STATEMENT (of the abstract entered in Block 20, if different from Report)

18. SUPPLEMENTARY NOTES

19. KEY WORDS (Continue on reverse side if necessary and identify by block number)

alpha phase
beta phase
martensite transformation
interface phase
lattice shears
slip systems

20. ABSTRACT (Continue on reverse side if necessary and identify by block number)

The occurrence of the interface phase in (α+β) titanium alloys is reviewed, and it is shown that the observed f.c.c. structure and orientation relationship may be explained either by appropriate choices of lattice shears in the β phase followed by atomic shuffles or by application of the Bowles-Mackenzie phenomenological theory of martensite transformations. In particular, the two orientation relationships which are reported

DD FORM 1 JAN 73 1473 EDITION OF 1 NOV 65 IS OBSOLETE

SECURITY CLASSIFICATION OF THIS PAGE (When Data Entered)

to occur between the interface phase and the lattice are rationalised in terms of variations in the principal lattice strain which in turn arises from variations in the β lattice parameter with solute content.

On the basis that the α and β lattices occur in the Burgers orientation relationship, it is shown that of all the possible α and β slip and twinning systems, four variants of a-type slip systems in α are parallel to β slip systems (systems B,R,S and E, Ref. 13) and two variants of (c+a)-type slip systems in α are parallel to β twinning systems. Introduction of the interface phase restricts slip across the interface to only two variants (E R for one orientation of the interface phase, S R for the other) for which there are parallel or closely parallel f.c.c. slip systems.

Transmission electron microscopy of Ti-1.8%Mn and Ti-3.9%Mn alloys heat-treated to provide a structure consisting of Widmanstatten α platelets in a β matrix and strained up to 6% in compression showed (i) that the interface phase occurred in the polycrystalline form and (ii) that it appeared to act as a barrier to slip from α to the β phase. However, it is considered that the effectiveness of the interface phase, γ , in these alloys in providing a barrier to slip arises primarily from its fine polycrystalline structure.

THE PROPAGATION OF SLIP ACROSS α / β INTERFACES IN TITANIUM ALLOYS

C. HAMMOND AND H. MARGOLIN

Department of Physical and Engineering Metallurgy
Polytechnic Institute of New York

CONTENTS

Abstract

The occurrence of the interface phase in (α-β) titanium alloys is reviewed, and it is shown that the observed f.c.c. structure and orientation relationship may be explained either by appropriate choices of lattice shears in the β phase followed by atomic shuffles or by application of the Bowles-Mackenzie phenomenological theory of martensite transformations. In particular, the two orientation relationships which are reported to occur between the interface phase and the lattice are rationalised in terms of variations in the principal lattice strain which in turn arises from variations in the β lattice parameter with solute content.

On the basis that the α and β lattices occur in the Burgers orientation relationship, it is shown that of all the possible α and β slip and twinning systems, four variants of a-type slip systems in α are parallel to β slip systems (systems B,R,S and E, Ref. 13) and two variants of (c + a)-type slip systems in α are parallel to β twinning systems. Introduction of the interface phase restricts slip across the interface to only two variants (E R for one orientation of the interface phase, S R for the other) for which there are parallel or closely parallel f.c.c. slip systems.

Transmission electron microscopy of Ti-1.8%Mn and Ti-3.9%Mn alloys heat treated to provide a structure consisting of Widmanstatten α platelets in a β matrix and strained up to 6% in compression showed (i) that the interface phase occurred in the polycrystalline form and (ii) that it appeared to act as a barrier to slip from α to the β phase. However, it is considered that the effectiveness of the interface phase, γ, in these alloys in providing a barrier to slip arises primarily from its fine polycrystalline structure.

(A) INTRODUCTION

The existence of an 'interface phase' at α/β boundaries in titanium alloys was first reported by Rhodes and Williams (1) in Ti-6%Al-4%V who found that it occurred either as a 'monolithic' single crystal layer with an f.c.c. structure ($a \approx 426$ pm) or as a striated layer ~200 μm thick consisting of platelets which gave rise to selected area diffraction patterns with arced reflections characteristic of the so-called "Type 2α" (2) (hexagonal α phase which is not related to the β by the Burgers orientation relationship.) The occurrence of these two types of interface phase appeared to be related to cooling rate, i.e. the rate of growth of Widmanstatten α plates into the retained β; the f.c.c. form being apparently favoured by slower cooling rates. Hall (3) working with the same alloy confirmed the existence of both phases and established an orientation relationship between the α, β and monolithic (γ) phases as:-

$$(0001)_\alpha // \{111\}_\gamma // \{110\}_\beta$$
$$\langle 11\bar{2}0\rangle_\alpha // \langle \bar{1}10\rangle_\gamma // \langle 1\bar{1}1\rangle_\beta$$

where the γ structure was either f.c.c. ($a \approx 436$pm or f.c.t. ($a \approx 432$ pm, $c/a = 1.13$) depending upon heat treatment. The hexagonal structure of the striated (p) form in slowly cooled material was often, though not always, related to the primary α by the orientation relationship.

$$(10\bar{1}0)_\alpha // (10\bar{1}0)_p$$
$$[0001]_\alpha // \langle \bar{1}\bar{3}13\rangle_p$$

The existence of the interface phase was also reported to occur in Ti-4% Mn and Ti-6%Al-2%Sn-4%Zr-6%Mo alloys (4) heat treated to produce a structure consisting of both equiaxed and Widmanstatten α plates. In these alloys the structure of the interface phase was reported as α (hexagonal) in a $\{10\bar{1}1\}$ twin orientation to the parent α plate. However, in more recent work (5) (6) it has been found that the interface phase had the f.c.c. (or possibly f.c.t.) structure irrespective of whether it occurred in the

'monolithic' or 'striated' form, the striations now being recognised as {111} twins, Hallam & Hammond (6) working with the near α' alloy Ti-6%Al-5%Zr-0.5%Mo-0.23%Si-0.02%Fe, distinguished three morphological forms - the monolithic (single crystal); {111} twinned, and polycrystalline, the latter form apparently being favoured by slower cooling rates. The lattice parameter was found to be 435 pm and the orientation relationship:-

$$(0001)_\alpha // \{001\}_\gamma // \{110\}_\beta$$
$$\langle 11\bar{2}0\rangle_\alpha // \langle 110\rangle_\gamma // \langle 1\bar{1}1\rangle_\beta$$

For the polycrystalline form, several variants of the above γ'-β orientation relationship were observed, the most dominant of which only possessed the above α'-γ orientation relationship.

The literature summarised above gives a very fragmentary account of the mode of formation, morphology and crystallography of the interface phase. Firstly, the structure has been established only on the basis of electron diffraction patterns which, because of the faint diffuse or streaked spots that are generally observed, leads to considerable uncertainty in lattice parameter determinations. The possibility of establishing the structure using x-ray diffraction has been vitiated because (a) the interface phase occurs only in small volume fractions (< 2% in the alloys studied to date) (b) It is highly dislocated (leading to the diffuse electron diffraction spots) and hence broadened x-ray reflections and (c) the f.c.c. d-spacings coincide closely with α (hexagonal) d-spacings and hence would be obscured in the much more intense α x-ray diffraction peaks. Similarly, attempts have been made to relate the morphology and thickness of the interface phase to variations in heat treatment - interrupted cooling, cooling at different rates etc. The results to date have, however, by no means been conclusive. What is certain is (a) that the interface phase forms from the β during cooling and does not develop during isothermal holding

at elevated temperatures and (b) does not form at the α (martensitic)/β interfaces in quenched structures. It therefore appears to be an intermediate phase which is associated with the transformation of β to α at a moving α/β interface.

A more important question is concerned with the effects of the interface phase on mechanical properties; in particular its effect (a) upon slip propagation across the interface, (b) on void nucleation and growth at the interface during conditions of tensile loading or low cycle fatigue and (c) fracture characteristics.

Rhodes and Paton (7) attempted to relate interface phase width to the room temperature tensile properties of Ti-6%Al-4%V - not a straightforward task since manipulation of interface phase width also results in changes in volume fraction of the primary α. Their results do however indicate that elongation is reduced by increasing interface phase width up to 250 μm and that yield strength is increased by increasing interface phase width above 250 μm - i.e. that the interface phase acts as a barrier to slip. Brown and Smith (8) investigated fatigue crack initiation in Ti-6%Al-4%V with an aligned α' microstructure but found that for fatigue lives between 10^4 and 10^5 cycles the interface phase had no measurable effect.

Similarly, Northwood and Dosen (9) failed to detect any effect of interface phase on ductility and fracture strength in 'Excel', a Zr-3.35% Sn-0.85%Mo-0.8%Nb alloy heat treated in the β and (α + β) phase fields - changes in ductility and strength in certain temperature ranges could be associated with the onset of ω formation rather than the presence of interface phase. Hence, the question of the effect of the interface phase on slip propagation and the implications for void formation, fatigue and fracture characteristics, is by no means answered.

It was decided to approach the problem of the effect of the interface phase on slip propagation from two directions. Firstly, a crystallographic analysis of the reported orientation relationships between the interface phase and β and the parallelisms between variants of all the possible slip systems in α, f.c.c. and β and secondly an electron microscop study of slip propagation in α + β alloys that had been lightly deformed in compression.

(B) ALLOYS & EXPERIMENTAL TECHNIQUES

The alloys chosen for study were Ti-1.8%Mn and Ti-3.9%Mn, solutio treated in the β field at 900°C for 1/2 hour, furnace cooled to 700°C (to precipitate Widmanstatten α plates and the interface phase), held at this temperature for 24 hours (to equilibrate the structure) and water quenched. This heat treatment produced Widmanstatten α plates 3-4 μm thick in a retained β matrix of composition 11% Mn. The phase proportions were 18% β, 82% α (in the Ti-1.8%Mn alloy) and 37% β, 63% α (in the Ti-3.9% Mn alloy). The specimens in the form of 6mm diameter rods were deformed 1%, 5% and 6% in compression. They were then machined down to 3mm diameter rods and discs 1mm thick were then sliced from the rods using either a water-cooled slitting wheel or by spark-machining. The discs were then ground down to a thickness of ∿100 μm using fine silicon carbide paper, care being taken not to introduce deformation in the process. Thin foils were then prepared by the two stage jetting and polishing method. The first stage consists of 'jetting' each surface of the disc (which is mounted on a stainless steel gauze) with a stream of electrolyte. If the correct conditions of electrolyte flow rate, voltage and stream diameter are achieve a dish-shaped profile on each surface will be obtained. The specimen is then final polished in a bath of electrolyte, the process being stopped

immediately on perforation - the object being to obtain a small hole in the centre of the specimen which is surrounded by a thin area. The advantages of this technique over the "window" or 'Bollman" methods are (1) it obviates the necessity of cutting the thinned specimens (2) the thick rim around the central perforation can stabilize the specimen against possible spontaneous transformation and (3) the jetting process removes any surface deformation introduced during the grinding process.

The polishing solutions used initially were:-

295 ml methanol 175 ml butoxyethanol 30 ml percholoric acid	'Jetting' solution at room temperature and ∿120 volts.
295 ml methanol 175 ml butoxethanol 6 ml perchloric acid	'Final polishing' solution at <-40°C and 6∿12 volts.

These solutions, which have been used for a wide range of α, α + β and β titanium alloys, were completely unsuccessful for the Ti-Mn alloys and it was found impossible to control the conditions to avoid etching on the one hand and pitting on the other.

Hence, the polishing solutions used finally were:-

300 ml methanol 30 ml sulphuric acid	'Jetting' solution at room temperature and ∿70 volts.
300 ml methanol 15 ml sulphuric acid	'Final polishing' solution at <-50°C and ∿12 volts.

These solutions gave rise to brightly polished specimens but which, under the electron microscope, were frequently covered with a thin amorphous or finely crystalline oxide film. It is not clear from which stage of the specimen preparation process this oxide film arose. Attempts were made to clean the specimens by immersing them in concentrated nitric acid but this technique was not successful in removing the oxide film.

The specimens were examined in a JEM 120 electron microscope operating at 120KV. This microscope is fitted with a top entry specimen

stage which is capable of ($\pm$ 10°) tilt, and the selected area diffraction blades are approximately in focus at a magnification of 12K.

(C) RESULTS

(1) The Crystallography of the Interface Phase

It is now recognised that the interface phase in all its three morphologies has f.c.c. or f.c.t. structure and the attempts to describe it as α in a $\{10\bar{1}1\}$ or $\{10\bar{1}2\}$ twin orientation to the matrix ar probably mistaken. However, the question remains as to why the interfa phase should show two apparently distinct orientation relationships he β (from which it forms) and hence also α.

One approach is to consider possible shear mechanisms which transform the b.c.c. structure to the f.c.c. structure in the observed orientation relationship.

Case (a) A shear of $\tan^{-1} a\sqrt{2}/\frac{a}{\sqrt{2}} = \tan^{-1}\frac{1}{3} = 18.5°$ on a {11 plane in a $\langle 1\bar{1}0\rangle$ direction (i.e. the passage of a $a/6$ $\langle 1\bar{1}0\rangle$ dislocation across every {110} plane will generate an atomic arrangement close to f.c.c. as shown in Figs. 1a and b. Lattice distortions as indicated will then give rise to the f.c.c. structure which, on the variant of the shear system shown in Fig. 1 is

$$\begin{matrix}(011)_{bcc}//(111)_{fcc} \\ [\bar{1}\bar{1}1]_{bcc}//[\bar{1}01]_{fcc}\end{matrix} \qquad \text{(Case (a))}$$

This shear mechanism is of course nothing more than the 'inverse' of the Kurdjumov-Sachs mechanism proposed to describe the crystallography of the austenite to martensite transformation in steels.

Case (b) A twinning shear on every alternate $\{112\}_{bcc}$ plane generates a fine stack of $\{112\}_{bcc}$ twins. As shown by Hallam and Hammond (6) the atomic arrangement of this fine stack of twins is approximately

f.c.c. and small distortions and shuffles will generate the f.c.c. structure. For the particular variant of the twinning system:-

$$(112)\ [\bar{1}\bar{1}1]_{bcc}$$
$$\text{parallel to } (101)\ [\bar{1}01]_{fcc}$$

The predicted orientation relationship is:-

$$(\bar{1}10)_{bcc}//(010)_{fcc}$$
$$[\bar{1}\bar{1}1]_{bcc}\ [\bar{1}01]_{fcc} \qquad \text{(Case (b))}$$

These mechanisms are incomplete insofar as they ignore the nature of the "distortions" which are required to produce the final f.c.c. structure and the requirements for an undistorted interface plane. They do suggest however that the two f.c.c. orientations may be associated with different shear processes in the β and α ;

In Case (a) $(011)_\beta//(111)_{fcc}//(0001)_\alpha$ - i.e. basal slip in α

In Case (b)
(See Ref. (6):- $(112)_\beta//(101)_{fcc}//\{10\bar{1}0\}_\alpha$ - i.e. prism slip in α

It is however suggested that the question may be answered more comprehensively in terms of an analysis of the $\beta \rightarrow$ f.c.c. transformation in terms of the phenomenological theory of martensite transformation. Although the $\beta \rightarrow$ f.c.c. transformation is clearly not diffusionless, martensite theory has been successful in describing the crystallography (habit plane and orientation relationships) of other transformations in which diffusional processes occur.

The first stage in the analysis is to establish the correspondence between the b.c.c. and f.c.c. lattices.

The correspondence chosen is illustrated in Fig. 2 and this involves the smallest distortions required to transform the b.c.c. lattice to the f.c.c. lattice. It is simply the inverse of the Bain correspondence for the austenitic → martensite transformation in steels. The lattice stra: such that:-

$$a_\beta \rightarrow a_{fcc} \text{ in the } [001]_\beta // [001]_{fcc} \text{ direction and}$$

$$\sqrt{2}a_\beta \rightarrow a_{fcc} \quad \text{normal to the } [001]_\beta // [001]_{fcc} \text{ direction}$$

and is described by the principal lattice strains:-

$$P_1 = \frac{a_{fcc}}{\sqrt{2}a_\beta}, \quad P_2 = \frac{a_{fcc}}{a_\beta}$$

In general $P_1 < 1$ and $P_2 > 1$. The precise values depend of course on the ratios of the b.c.c. and f.c.c. lattice parameters. In the case of steels typical values of $a_{bcc} = 287$ pm and $a_{fcc} = 356$ pm give $P_1 = 0.88$, however, in the case of titanium alloys P_1 values are much closer to unity, e.g. for $a_\beta = 320$ pm and $a_{fcc} = 420 \sim 450$ pm, $P_1 = 0.93 \sim 0.99$. When P_1 is unity the $(001)_\beta // (001)_{fcc}$ plane is the undistorted or invariant plane of the transformation; it is identified with the habit plane and the β and the f.c.c. crystals exist in the 'Bain' orientation relationship:-

$$(001)_\beta // (001)_{fcc}$$

$$[110]_\beta // [100]_{fcc}$$

For the general case where $P_1 < 1$, the lattice (Bain) strain is no longer an invariant plane strain. If however the lattice strain is accompanied by a lattice invariant shear (L.I.S.) (of a magnitude that can be calculated), the total strain of the transformation (lattice strain plus L.I.S.) is an invariant plane strain and the invariant plane is identified with the habit plane of the transformation. The invariant planes

f.c.c. and small distortions and shuffles will generate the f.c.c. structure. For the particular variant of the twinning system:-

$$(112)\ [\bar{1}\bar{1}1]_{bcc}$$
$$\text{parallel to } (101)\ [\bar{1}01]_{fcc}$$

The predicted orientation relationship is:-

$$(\bar{1}10)_{bcc}//(010)_{fcc}$$
$$[\bar{1}\bar{1}1]_{bcc}\ [\bar{1}01]_{fcc} \qquad \text{(Case (b))}$$

These mechanisms are incomplete insofar as they ignore the nature of the "distortions" which are required to produce the final f.c.c. structure and the requirements for an undistorted interface plane. They do suggest however that the two f.c.c. orientations may be associated with different shear processes in the β and α ;

In Case (a) $(011)_{\beta}//(111)_{fcc}//(0001)_{\alpha}$ - i.e. basal slip in α

In Case (b)
(See Ref. (6):- $(112)_{\beta}//(101)_{fcc}//\{10\bar{1}0\}_{\alpha}$ - i.e. prism slip in α

It is however suggested that the question may be answered more comprehensively in terms of an analysis of the $\beta \rightarrow$ f.c.c. transformation in terms of the phenomenological theory of martensite transformation. Although the $\beta \rightarrow$ f.c.c. transformation is clearly not diffusionless, martensite theory has been successful in describing the crystallography (habit plane and orientation relationships) of other transformations in which diffusional processes occur.

The first stage in the analysis is to establish the correspondence between the b.c.c. and f.c.c. lattices.

The correspondence chosen is illustrated in Fig. 2 and this involves the smallest distortions required to transform the b.c.c. lattice to the f.c.c. lattice. It is simply the inverse of the Bain correspondence for the austenitic → martensite transformation in steels. The lattice stra: such that:-

$$a_\beta \rightarrow a_{fcc} \text{ in the } [001]_\beta // [001]_{fcc} \text{ direction and}$$

$$\sqrt{2}a_\beta \rightarrow a_{fcc} \quad \text{normal to the } [001]_\beta // [001]_{fcc} \text{ direction}$$

and is described by the principal lattice strains:-

$$P_1 = \frac{a_{fcc}}{\sqrt{2}a_\beta}, \quad P_2 = \frac{a_{fcc}}{a_\beta}$$

In general $P_1 < 1$ and $P_2 > 1$. The precise values depend of course on the ratios of the b.c.c. and f.c.c. lattice parameters. In the case of steels typical values of $a_{bcc} = 287$ pm and $a_{fcc} = 356$ pm give $P_1 = 0.88$, however, in the case of titanium alloys P_1 values are much closer to unity, e.g. for $a_\beta = 320$ pm and $a_{fcc} = 420 \sim 450$ pm, $P_1 = 0.93 \sim 0.99$. When P_1 is unity the $(001)_\beta // (001)_{fcc}$ plane is the undistorted or invariant plane of the transformation; it is identified with the habit plane and the β and the f.c.c. crystals exist in the 'Bain' orientation relationship:-

$$(001)_\beta // (001)_{fcc}$$

$$[110]_\beta // [100]_{fcc}$$

For the general case where $P_1 < 1$, the lattice (Bain) strain is no longer an invariant plane strain. If however the lattice strain is accompanied by a lattice invariant shear (L.I.S.) (of a magnitude that can be calculated), the total strain of the transformation (lattice strain plus L.I.S.) is an invariant plane strain and the invariant plane is identified with the habit plane of the transformation. The invariant planes

of the product and parent lattices are not parallel, a rotation is required to bring them into coincidence and it is this rotation (away from the 'Bain' orientation relationship of Fig. 2) which gives rise to the observed orientation relationship.

The lattice invariant shear is usually taken to be a slip or twinning shear in either the product or the parent lattices. In the case of steels and iron base alloys two L.I.S. systems have been identified (10).

System I - corresponding to twinning in the b.c.c./b.c.t. phase (martensite) which on the above variant of the correspondence is:-

$$(112)\ [\bar{1}11]_{bcc}$$

$$(101)\ [\bar{1}01]_{fcc}$$

System II - corresponding to faulting or twinning in the f.c.c. phase (austenite) which on the above variant of the correspondence is:-

$$(111)\ [11\bar{2}]_{fcc}$$

$$(011)\ [01\bar{1}]_{bcc}$$

Shear System I describes the crystallography of the "{259}" habit plane martensites in (for example) Fe-1.78%C, Fe-22%Ni-0.8%C and Fe-31%Ni alloys and Shear System II describes the crystallography of the martensites in low stacking fault energy stainless steels, for example Fe-17%Cr-9%Ni and Fe-12%Mn-10%Cr-4%Ni (10).

It is seen immediately that System I corresponds to the shear analysis in case (b) above and System II corresponds to the shear analysis in case (a). In the present case, the observation that the f.c.c. phase is frequently twinned suggests that Shear System II is operative. This system has been previously used to describe the f.c.c. martensite transformation

in Ti-5%Mn alloys (11) and a stereogram showing the results of the analysis is shown in Fig. 3 which should be compared with Fig. 2. The arrows indicate the directions in which the habit plane normal and $\{100\}_{f.c.c.}$ poles move (as a result of the rotation required to bring the invariant planes into coincidence) and the scale markings along these arrows indicate decreasing values of P_1 from 1.0, 0.99, 0.98 etc., it can be seen immediately that the $(010)_{f.c.c.}$ pole moves only a small angle from $(\bar{1}10)_\beta$, the $(111)_{f.c.c.}$ pole moves towards $(011)_\beta$ and the $(\bar{1}01)_{f.c.c.}$ pole moves towards $(\bar{1}\bar{1}1)_\beta$. The Kurdjumov-Sachs orientation relationship is then a statement of the parallelism of the poles (or directions):-

$$\begin{matrix}(011)_\beta // (111)_{f.c.c.} \\ [\bar{1}\bar{1}1]_\beta // [\bar{1}01]_{f.c.c.}\end{matrix} \qquad (a)$$

which is, of course, the orientation relationship that it closely obeyed for austenite → ferrite transformation.

For the β→ f.c.c. transformation in titanium alloys, it can be seen that since the P_1 values are closer to unity and because of the inherent inaccuracy of orientation relationship determinations by electron diffraction, the orientation relationship may be stated as:-

$$\begin{matrix}(\bar{1}10)_\beta // (010)_{f.c.c.} \\ [\bar{1}\bar{1}1]_\beta // [\bar{1}01]_{f.c.c.}\end{matrix} \qquad (b)$$

Footnote

It is important to note that the particular variants of the correspondence, orientation relationships and shear systems quoted in the section C.1 in the text and illustrated in figures 1-3 have been chosen to be entirely self-consistent.

These orientation relationships (a) and (b) are of course the orientation relationships quoted for the interface phase and are seen to differ by only a few degrees. Furthermore, the analysis predicts that the larger the observed f.c.c. lattice parameter, i.e. the larger the P_1 values, the more closely does the orientation relationship coincide with (b). Examination of the literature appears to confirm this. For example, Rhodes & Paton (5) find that in the Ti-6%Al-4%V alloy $a_{f.c.c.}$ = 426 pm and that the Kurdjumov-Sach orientation relationship (a) is obeyed. Hallam and Hammond (6) find that in the Ti-6%Al-5%Zr-0.5Mo-0.23%Si alloy $a_{f.c.c.}$ = 435 pm and that orientation relationship (b) is confirmed. It is hoped that further measurements of β and f.c.c. lattice parameter relationships will be made to check the analysis.

A further prediction of the analysis is that interface phase which forms at different temperatures in a given alloy may show different orientation relationships. The lower the temperature in the α+β phase field, the more solute-rich is the β from which the interface phase forms. Since β stabilizing alloying elements reduce the β lattice parameter, then for a given f.c.c. lattice parameter P_1 will be lower at lower temperature and hence the interface phase in orientation (a) will tend to occur. In continuous cooling conditions where the interface phase nucleates across a whole temperature range a whole range of orientations would be expected to occur.

With regard to the effect of the interface phase on slip propagation across the interface, it would be expected that slip propagation would not be affected differently by the two similar orientations and in this sense the distinction is not important. However, the analysis of parallelism of slip systems in α, β and f.c.c. has also been carried out on the basis that orientation (b) occurs as a different <u>variant</u> which may only be converted to variant (a) by a large rotation.

This appears in fact to be case. Consider for example the particular variant of the β/f.c.c./α orientation relationship (a);

$$(011)_\beta // (111)_{f.c.c.} // (0001)_\alpha$$

$$[\bar{1}\bar{1}1]_\beta // [\bar{1}01]_{f.c.c.} // [\bar{1}\bar{1}20]_\alpha$$

This variant in terms of orientation relationship (b) (see Fig. 3) is expressed as:-

$$(\bar{1}10)_\beta // (010)_{f.c.c.} // (\bar{1}101)_\alpha$$

$$[\bar{1}\bar{1}1]_\beta // [\bar{1}01]_{f.c.c.} // [\bar{1}\bar{1}20]_\alpha$$

Which is <u>not</u> the variant of the interface phase which has {100} f.c.c.//$(0001)_\alpha$.

C(2) Analysis of Slip in α and β and the interface Phase

The β slip and twinning systems are:-

{110} <111> (12 variants) } $\underline{b} = \underline{a}/_2$ <111>

{112} <111> (24 variants) }

The dominant α slip systems are:-

(0001) $\langle 11\bar{2}0 \rangle$ (3 variants) }

$\{10\bar{1}0\}$ $\langle 11\bar{2}0 \rangle$ (3 variants) } $\underline{b} = \underline{a}$

$\{10\bar{1}1\}$ $\langle 11\bar{2}0 \rangle$ (6 variants) }

$\{11\bar{2}2\}$ $\langle 11\bar{2}3 \rangle$ (6 variants) $\underline{b} = (\underline{a} + \underline{c})$

The f.c.c. slip and twinning systems are:-

{111} <110> (12 variants)

{111} <112> (12 variants)

Consider first parallelism between slip systems in the α and β phases (no interface phase present) for the particular variant of the Burgers orientation relationship:-

$$(110)_\beta // (0001)_\alpha$$
$$[1\bar{1}1]_\beta // [1\bar{2}10]_\alpha$$

For this variant of the orientation relationship the habit plane is $(\bar{3}34)_\beta // (\bar{5}140)_\alpha$. Fig. 4 shows that the parallel or closely parallael systems are:-

B:-	$(\bar{1}010)$	$[1\bar{2}10]_\alpha // (112)$	$[1\bar{1}1]_\beta$	} a slip in α
R:-	$(\bar{1}011)$	$[1\bar{2}10]_\alpha // (011)$	$[1\bar{1}1]_\beta$	
S:-	$(10\bar{1}1)$	$[1\bar{2}10]_\alpha // (10\bar{1})$	$[1\bar{1}1]_\beta$	
E:-	(0001)	$[1\bar{2}10]_\alpha // (110)$	$[1\bar{1}1]_\beta$	
	$(\bar{1}1\bar{2}2)$	$[\bar{1}\bar{1}23]_\alpha // (112)$	$[11\bar{1}]_\beta$	} (c + a) slip in α closely parallel (∿5°) to twinning in β
	$(\bar{1}\bar{1}22)$	$[11\bar{2}3]_\alpha // (112)$	$[11\bar{1}]_\beta$	

Hence, only 4 variants of a shear systems (labelled B, R, S, E) are parallel to slip or twinning systems in β and all have a common $[1\bar{2}10]_\alpha // [1\bar{1}1]_\beta$ shear direction which lies ∿11° from the habit plane. The two (c + a) slip systems are closely parallal to twinning systems in the β. The (c + a) dislocation has a complex core structure and consists of a zonal dislocation which produces a stacking fault shear in three successive planes plus three partial dislocations which annihilate the stacking faults (12). Depending on the direction of shear the stacking faults may either precede or follow the zonal dislocation.

The important consequence of this geometry is that the shear stress required to move the dislocation is asymmetric with respect to the shear direction, i.e. the shear stress required to glide the (c + a) dislocation on the $(11\bar{2}2)$ plane in the $[\bar{1}\bar{1}23]$ direction is less than the shear stress required to glide the dislocation in the opposite $[11\bar{2}\bar{3}]$ direction. In the present case it is of interest to note that the easy glide direction corresponds to the twinning (not the anti-twinning) direction in β.

The a slip systems are labelled B, R, S, Σ in accordance with the nomenclature of Ankem & Margolin (13) who have analysed the elastic interactions which occur at Widmanstattan α/β interfaces for 54 orientations of the stress axis with respect to the interface. The elastic shear stresses were resolved onto the basal, prism and pyramidal slip systems of the α phase in order to determine the effect of the resolved compatability shear strains on the initiation of slip in the two structures. The analysis was quite general for the 54 stresses chosen, all variants of basal, prism and pyramidal slip systems were considered, irrespective of whether they corresponded to slip systems in the β or not. In this work the habit plane was fixed as $(\bar{3}\bar{3}4)_\beta$ and two variants of the orientation relationship were considered:-

$$\begin{matrix}(110)_\beta // (0001)_\alpha \\ [1\bar{1}1]_\beta // [\bar{1}2\bar{1}0]_\alpha\end{matrix} \quad \text{which gives } (\bar{3}34)_\beta // (\bar{5}140)_\alpha$$

and

$$\begin{matrix}(110)_\beta // (0001)_\alpha \\ [\bar{1}11]_\beta // [\bar{2}110]_\alpha\end{matrix} \quad \text{which gives } (\bar{3}34)_\beta // (\bar{1}\bar{3}580)_\alpha$$

The first of these corresponds to the variant chosen above and is in accordance with the crystallographic relationships normally observed. Although most of the calculations were made on the basis of the second orientation relationship, it was found that the differences between the calculated elastic strains for the two orientation relationships were less than 5%.

The stress axes which give rise to strong or significant interactions have been identified from the paper of Ankem and Margolin (13) and are indicated in Fig. 4. The captions indicate the effect of β on opposing or aiding the initiation of slip in α. It will be seen that the interactions on basal and pyramidal slip systems are 'significant' or 'strong' and generally the stresses act in such a way that α slip in these systems is 'aided'

It is also of interest to identify the parellel slip and twin systems for the second orientation relationship, Fig. 5.

A $(01\bar{1}0)\ [\bar{2}110]_\alpha // (1\bar{1}2)\ [\bar{1}11]_\beta$

P $(0\bar{1}11)\ [\bar{2}110]_\alpha // (101)\ [\bar{1}11]_\beta$

Q $(0\bar{1}11)\ [\bar{2}110]_\alpha // (01\bar{1})\ [\bar{1}11]_\beta$

D $(0001)\ [\bar{2}110]_\alpha // (110)\ [\bar{1}11]_\beta$

The letters A, P, Q, D refer to the α slip systems of Ankem and Margolin (13) and in this case none of the 54 stress axes considered gave rise to strong 678 significant stress interactions for these systems. Hence, the elastic stress interactions are important only in the former case (Fig. 4) in which the a slip vector lies close to the interface plane.

The effect of the interface phase on the propagation of slip will now be considered. As shown above, there are two orientation relationships which, on the basis of the martensite analysis described above, differ by only a few degrees. Close parallelism between the same variants of α, f.c.c. and β slip and twinning systems will therefore occur for the two f.c.c. orientations which would therefore be expected to have the same effect upon slip propagation across the interface. However, the analysis has been generalised on the basis that the two f.c.c. orientations are distinct, viz

$$(110)_\beta // (0001)_\alpha // (111)_{fcc}$$

$$[\bar{1}1\bar{1}]_\beta // [1\bar{2}10]_\alpha // [0\bar{1}1]_{f.c.c.}$$

and

$$(110)_\beta // (0001)_\alpha // (001)_{fcc}$$

$$[\bar{1}1\bar{1}]_\beta // [1\bar{2}10]_\alpha // [\bar{1}\bar{1}0]_{f.c.c.}$$

For the first of these orientations:-

E $(110)_{\beta}//(0001)_{\alpha}//(111)_{fcc}$

R $(011)_{\beta}//(\bar{1}011)_{\alpha} \sim 10^{\circ}$ from $(\bar{1}11)_{fcc}$

and for the second:-

S $(10\bar{1})_{\beta}//(10\bar{1}1)_{\alpha} \sim 10^{\circ}$ from $(1\bar{1}1)_{fcc}$

R $(011)_{\beta}//(\bar{1}011)_{\alpha} \sim 10^{\circ}$ from $(\bar{1}11)_{fcc}$

Hence, in either case there are two parallel or closely parallel slip systems in α, the interface phase and β.

This analysis is only applicable, or useful for the case where <u>one</u> variant of the interface phase (the 'monolithic' form) occurs. For the polycrystalline form many f.c.c. shear systems will be found to be parallel or closely parallel to the α and β shear systems and therefore any effect which the interface phase may have on inhibiting slip propagation will not arise from the crystallography, but will arise rather from the interactions which occur when dislocations moving from the β or α meet a fine-grained polycrystalline structure.

3) Electron Microscopy of the Interphase Phase

The results described in this section are less extensive than hoped partly because of the electropolishing problems discussed above. Further work was carried out in the U.K. on the remaining available material and using the Philips EM300 electron microscope at the Department of Metallurgy, University of Leeds and the 1MV A.E.I. high voltage microscope at the British Steel Corporation Research Laboratories at Sheffield, but with little more success. However, it should be noted that further non-Mn containing $\alpha + \beta$ alloys have subsequently been procured and it anticipated that the project will be pursued in the future at the University of Leeds as part of M.Phil or M.Sc. research projects. Copies of such project reports will be made available.

Ti-1.8%Mn, Deformed 1%

As discussed above (Section B) the alloy was heat treated to produce a distribution of Widmänstatten and grain boundary α with 18% untransformed β. The α phase showed a uniform distribution of tangled dislocations (Fig. 6) which were probably inherited from the $\beta \rightarrow \alpha$ transformation. Dark field analyses showed that these dislocations had a type Burgers vectors. Fig. 7 is a dark field micrograph using $\{10\bar{1}1\}_\alpha$ reflection and Fig. 8 is a dark field micrograph using an $(0002)_\alpha$ reflection in which the dislocations are out of contrast. Figs. 6 and 8 also show a low volume fraction of precipitates or inclusions. Although these appear to be strongly diffracting in Fig. 8, no 'extra' spots could be detected in the electron diffraction patterns from which an identification could be made. Many regions of the foils showed no such particles and it is supposed that they are inclusions.

Fig. 9 shows the interface between α and β and the interface phase which appears to consist of small platelets at an angle to the boundary - i.e. the "polycrystalline" form and Fig. 10 is a dark field micrograph of the same area. It is clear, particularly from Fig. 10 that the interface phase has grown into the β as expected. What is surprising in this case is that the β/interface phase interface is smooth.

Figs. 11 and 12 show similar structures, in particular (Fig. 12) the irregular nature of the interface phase platelets. it is possible that Fig. 12 shows the "f.c.c. twinned" form since about half the platelets appear to be in contrast but the diffraction patterns could not confirm this The "speckly" contrast within the platelets are probably Bragg (bend) contours indicating distortion within the platelets themselves.

In order to observe the effect of the interface phase on slip propagation, it is important that the compression should give rise to a fairly high density of clearly discernible slip bands. It became evident that 1% compressive strain had not generated slip bands in sufficient numbers for them to be detected in the small areas available for observation in the thin foils a problem which was exacerbated in the present case becaus of the electropolishing problem. Hence specimens deformed 5% and 6% (1% plu an additional 5%) were examined.

Ti-1.8%Mn, deformed 5%

Fig. 13 shows that the density of dislocation tangles in the α phase has increased (cf Fig. 6) and that a proportion of the dislocations have a $\underline{c}$ + $\underline{a}$ type Burgers vector as shown by the dark field micrograph (Fig. 14) taken using an $(0002)_\alpha$ reflection (cf Fig. 8). The dislocations also lie on fairly well defined slip bands (Fig. 15) which trace analysis generally indicated as $\{10\bar{1}1\}_\alpha$.

Fig. 16 is a dark field micrograph using a $\{110\}_\beta$ (includes a $\{111\}_{fcc}$) reflection and shows a central band of retained β with one variant of the interface phase in contrast. Within the β are clearly defined slip traces which trace analyse to $\{112\}_\beta$ (trace A) and $\{112\}_\beta$ or $\{110\}_\beta$ (traces B and C). Fig. 17 is a dark field micrograph (slightly displaced from Fig. 16) taken using a $\{10\bar{1}1\}_\alpha$ reflection.

Electron diffraction showed that the α and β lattices existed in the expected Burgers orientation relationship and the interface phase in the orientation relationship (a) (page 10). The α/β habit plane was confirmed to be the $\{334\}_\beta$ type. As can be seen from the above micrographs, there is no evidence of slip across the interface phase.

Ti-1.8%Mn, deformed 6%

It was hoped that increased deformation would give a greater concentration of slip bands both in α and β from which the effect of the interface phase could be ascertained more clearly. Fig. 18 is a dark field micrograph using a $\{11\bar{2}0\}_\alpha$ reflection again showing α slip bands which appear to be arrested at the interface phase (which is out of contrast). Fig. 19 is a bright field micrograph, again showing α slip bands and the "petal like" surface oxide in the β phase. This oxidation problem, as mentioned above, effectively masked any β slip bands. In one case was clear evidence of deformation across the interface obtained (Fig. 20), but this shows a $\{10\bar{1}1\}_\alpha$ twin (not slip trace) extending across the central β phase region. Unfortunately the interface phase could not be brought into contrast because of the specimen tilting limitations

(D) CONCLUSIONS AND SUGGESTION FOR FUTURE WORK

The theoretical analysis of the crystallography of the interface phase in terms of the phenomenological theory of martensite transformations appears to be satisfactory and also to have an exact corollary with the (reverse) bcc → fcc transformation for Fe-Ni alloys (Appendix E). It also suggests the possibility that the observed orientatic relationship (a) or (b) (page 10) may be used to predict the temperature of formation of the interface phase, orientation (b) tending to occur at higher temperatures than orientation (a) (page 11). The analysis is unfortunately of no help in determining why different morphologies ('monolithic','twinned' or 'polycrystalline') of the interface phase occur.

The analysis of slip propagation across the interface phase is clearly much more complicated when this phase exists in the twinned or polycrystalline forms, as was indeed observed in the present alloys. The small crystallite sizes complicate and obscure the contrast of dislocations crossing the interface and the complex diffraction patterns vitiate Burgers vector analysis. It is therefore important to be able to select an alloy system and heat treatment which gives rise to the single crystal 'monolithic form where these problems can be avoided. It is hoped that this line of approach will be pursued in the future.

However, the analyses of Section C2 and the experimental results do suggest that the polycrystalline interface phase does act as a barrier to slip propagation even though the details of the mechanism, as discussed above, are not clear.

It is suggested that future work should concentrate on the Ti-Al-V alloy system since;

(1) Ti-6%Al-4%V gives rise, under certain heat treatment conditions, to the monolithic form of the interface phase.

(2) The oxidation problems which arise with manganese, will not occur.

(3) The presence of Al will suppress the $\beta \rightarrow \omega$ transformation.

(E) APPENDIX

ORIENTATION RELATIONSHIP VARIATIONS IN f.c.c. → b.c.c. FERROUS MARTENSITE TRANSFORMATIONS

The basic theory and data on which this Appendix is based is to be found in J.S. Bowles & J.K. Mackenzie "The Crystallography of Martensite Transformations III. Face Centered Cubic to Body Centered Tetragonal Transformations" (Ref. 14). The sketch below is an expanded version of Fig. 7 of this paper which refers to the special case of cubic martensites.

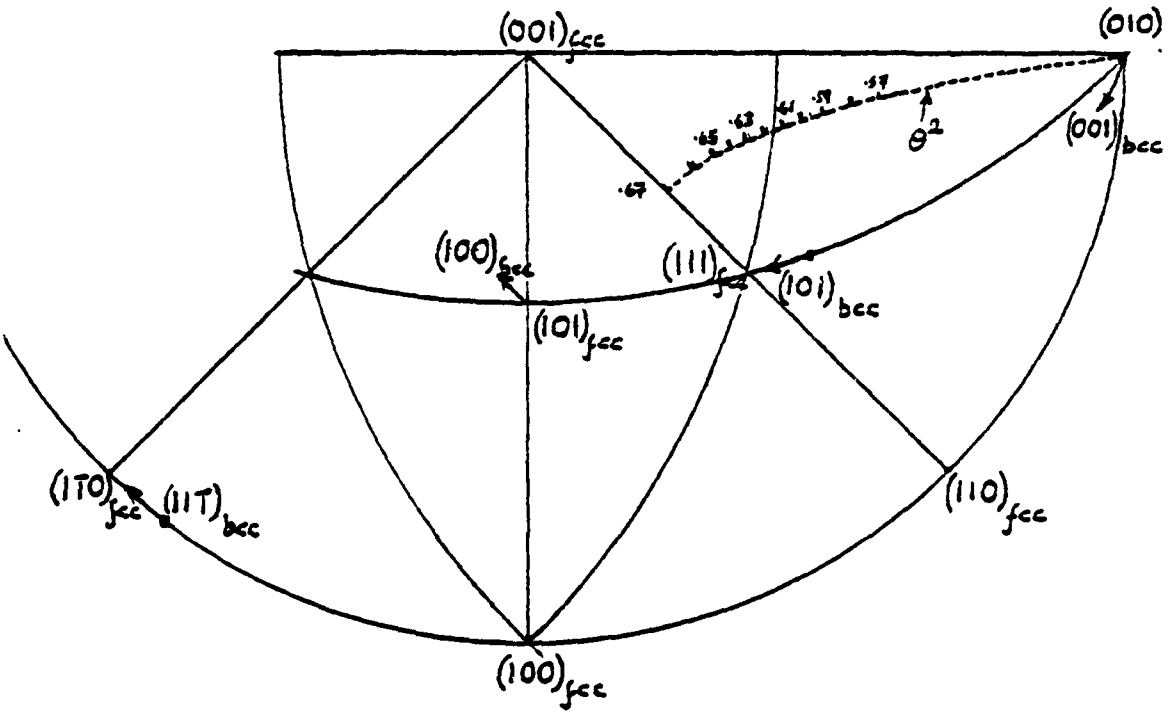

It should be noted that the variant of the correspondence for f.c.c. b.c.c. used by Bowles and Mackenzie is <u>different</u> from that used in Section C of this report. It is:-

$$\left(BC_{\bar{I}}\right) = \begin{pmatrix} 1 & 0 & 1 \\ 1 & 0 & \bar{1} \\ 0 & 1 & 0 \end{pmatrix}$$

The dashed line gives the predicted habit plane for cubic martensites for varying values of the parameter $\theta^2 = \delta^2 \left(\frac{a_{bcc}}{a_{fcc}}\right)^2$ where δ = dilatation parameter (assumed to be unity). The parameter θ (used by Bowles & Mackenzie), is related to P_1, the principal lattice strain as used in this report as follows:-

$$P_1 = \frac{a_{fcc}}{\sqrt{2}\, a_{bcc}} \qquad \therefore P_1 = \frac{1}{\sqrt{2}\,\theta}$$

$$\text{or } \theta^2 = \frac{1}{2P_1^2}$$

The following table gives a comparison of P_1 and θ^2 values.

P_1	θ^2
1.00	0.50
0.98	0.521
0.96	0.543
0.94	0.566
0.92	0.591
0.90	0.617
0.88	0.646
0.86	0.676
0.84	0.709

when $P_1 = 1$ ($\theta^2 = 0.5$) the LIS is zero and the b.c.c. and f.c.c. lattices exist in the Bain orientation relationship which on the above Bowles & Mackenzie variant of the correspondence is:-

$$(010)_{fcc}//(001)_{bcc}$$

$$(101)_{fcc}//(100)_{bcc}$$

and the habit plane is parallel to $(010)_{fcc}//(001)_{bcc}$. As P_1 decreases below 1 (and θ^2 increases above 0.5), the transformation is accomplished by the Bain strain plus an increasing lattice invariant shear. The lattices rotate away from the Bain orientation relationship as indicated by the arrowed b.c.c. poles in the diagram. Note in particular that as $(001)_{bcc}$ rotates away from $(101)_{fcc}$, $(101)_{bcc}$ rotates towards $(111)_{fcc}$ and $[1\bar{1}1]_{bcc}$ rotates towards $[1\bar{1}0]_{fcc}$ - giving, of course the Kurdjumov-Sachs orientation relationship. The Nishiyama orientation relationship $(101)_{bcc}//(111)_{fcc}$ and $[10\bar{1}]_{bcc}//[1\bar{2}1]_{fcc}$ is 'intermediate' between Bain and Kurdjumov-Sachs.

At the same time the habit plane moves along the dotted line. The calibration marks along this line give the predicted habit plane for a particular θ^2 value.

Comparison of Theory with Experiment

The θ^2 values for ferrous transformations are in the range 0.61-0.65, which is rather limited. Furthermore the tetragonality of carbon-containing martensites complicates the analysis - there is, for example, a different habit plane curve for each c/a ratio.

Thus the comparison can only be carried out in a straightforward manner for the bcc martensites - Fe-Ni and Fe-0%C. Using the data reproduc in Table 1 of Ref. 14.

Composition	$\theta^2(\delta=1)$
Fe-0%C i.e. Fe0%Ni	0.650
Fe-30%Ni	0.642
Fe-32.5%Ni	0.640

Hence, as the Ni content increases, θ^2 decreases, the habit plane would be expected to move along the curve to decreasing θ values and the orientationship would be expected to move in the general sense:-

Kurdjumov-Sachs → Nishiyama → Bain. This is indeed the case - the Fe-0%C transformation (and Fe-low C steels which have similar θ^2 values) shows (approximately) the Kurdjumov-Sachs orientation relationship and the Fe-Ni alloys show (approximately) the Nishiyama relationship. The θ^2 values are not of course sufficiently small (i.e. do not approach 0.5) for the predicted orientation relationship to become very close to Bain. Hence, it appears that the relationships between lattice parameter ratios, orientation relationships and habit planes discussed for the titanium alloys case apply in a similar way to the ferrous alloys case.

(F) REFERENCES

1) C.G. Rhodes & J.C. Williams: Met. Trans. 6A (1975) p.1670

2) C.G. Rhodes & J.C. Williams: Met. Trans. 6A (1975) p. 2103

3) I.W. Hall: Scand. J. Met. 8 (1979) p.17.

4) H. Margolin, E. Levine & M. Young: Met. Trans 8A (1977) p.373.

5) C.G. Rhodes & N.E. Paton: Met. Trans 10A (1979) p.209.

6) P. Hallam & C. Hammond: 4th Int. Conf. on Titanium, Kyoto (1980) Ed. H. Kumura and O. Izumi. Met. Soc. AIME (1980) p. 1435

7) C.G. Rhodes and N.E. Paton: Met. Trans 10A (1979) p.1753.

8) R. Brown & G.C. Smith: Abstract in Conference on "Modern Metallography in Metallurgy.Sheffield Sept. 1980 (Metals Society).

9) D.O. Northwood & K. Dosen: Ibid.

10) P.M. Kelly: Acta Met 13 (1965) p.635.

11) C. Hammond & P.M. Kelly: Acta Met. 17 (1969) p.869.

12) H.S. Rosenbaum: "Deformation Twinning" p.43 ed. Reed-Hill. Gordon & Breach N.Y. 1964.

13) S. Ankem & H. Margolin: Met. Trans 11A (1980) p.963.

14) J.S. Bowles & J.K. Mackenzie: Acta Met 2 (1954) p.224.

(G) ACKNOWLEDGMENTS

This work was supported by the Air Force Office of Scientific Research under Grant No. 79-0028 and the Office of Naval Research under contract N-00014-75-C-0793. The authors are grateful to Drs. Alan Rosenstein and Bruce MacDonald for their interest and support. The funds made available for this work permitted one the authors (C.H.) to come to the Polytechnic to carry out the research.

Figure 1(a). The 'inverse' Kurdjumov-Sachs mechanism for bcc → fcc transformation. A $(011)_{\beta}$ projection showing atom displacements resulting from an $a/6\ [0\bar{1}1]$ shear on every $(011)_{bcc}$ plane. The atoms in each successive $(011)_{bcc}$ plane are represented by O, X symbols. The first O layer of atoms is unchanged, the next X layer of atoms shifted $a/6\ [0\bar{1}1]$, the next layer shifted $a/6\ [0\bar{1}1] + a/6\ [0\bar{1}1] = a/3\ [0\bar{1}1]$ and so on.

INVERSE' KURDJUMOV-SACHS MECHANISM

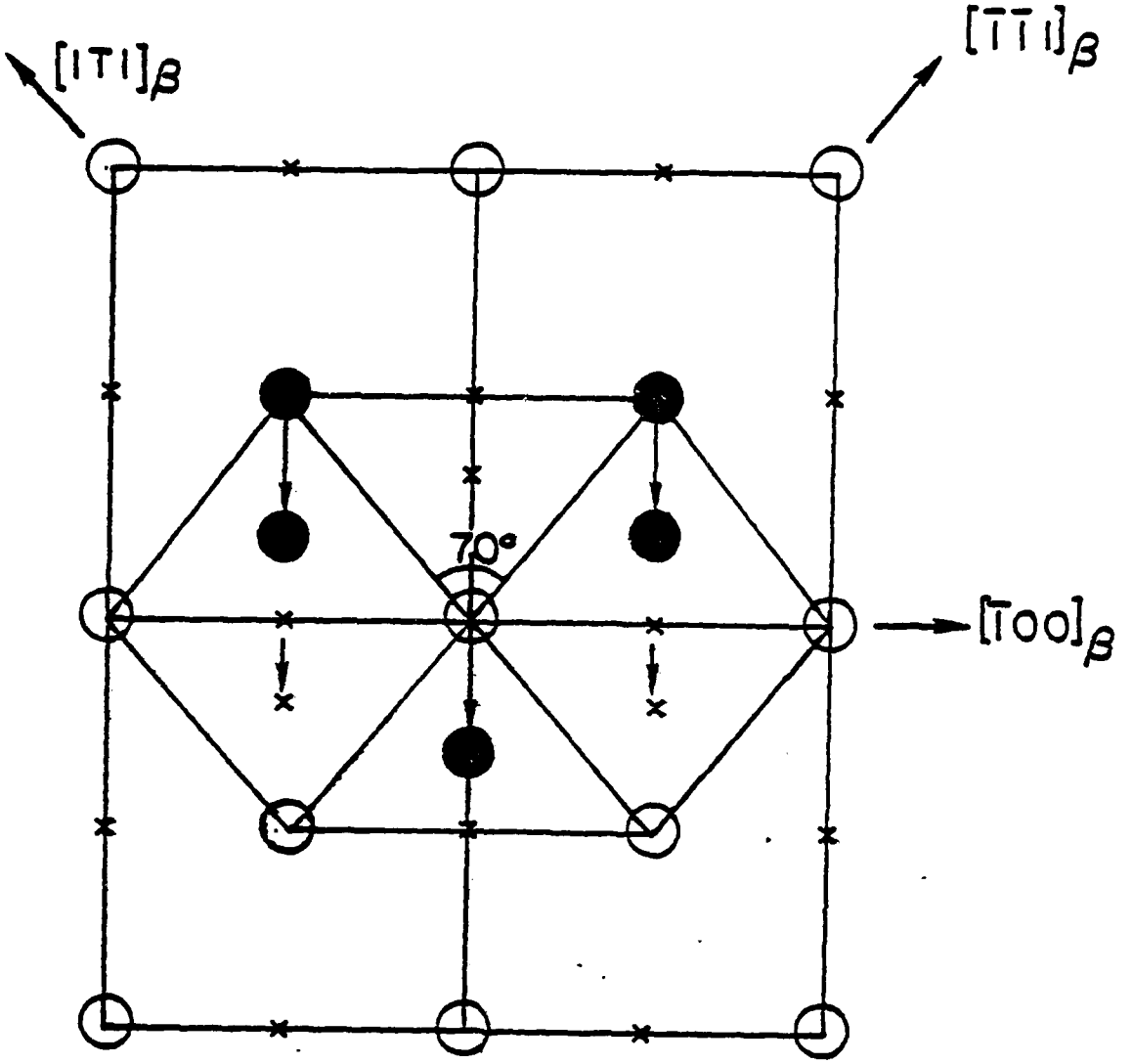

Shear (011) [0 $\bar{1}$ 1] $_\beta$

(a/6 [0 $\bar{1}$ 1] dislocations across

every (0 1 1)$_\beta$ plane)

Figure 1(b). A $(111)_{fcc}$ projection showing the resulting atom arrangement and "distorted fcc" cell (compare with Fig. 1a).
The additional strains to generate the fcc structu are:

$$\frac{a_{bcc}}{\sqrt{2}} \rightarrow \frac{a_{fcc}}{\sqrt{3}} \quad \text{in} \quad [011]_{bcc} // [111]_{fcc}$$

$$\sqrt{2}a_{bcc} \rightarrow \frac{\sqrt{6}}{2} a_{fcc} \quad \text{in} \quad [0\bar{1}1]_{bcc} // [11\bar{2}]_{fcc}$$

$$a_{bcc} \rightarrow \frac{a}{\sqrt{2}} \text{ fcc} \quad \text{in} \quad [\bar{1}00]_{bcc} // [\bar{1}10]_{bcc}$$

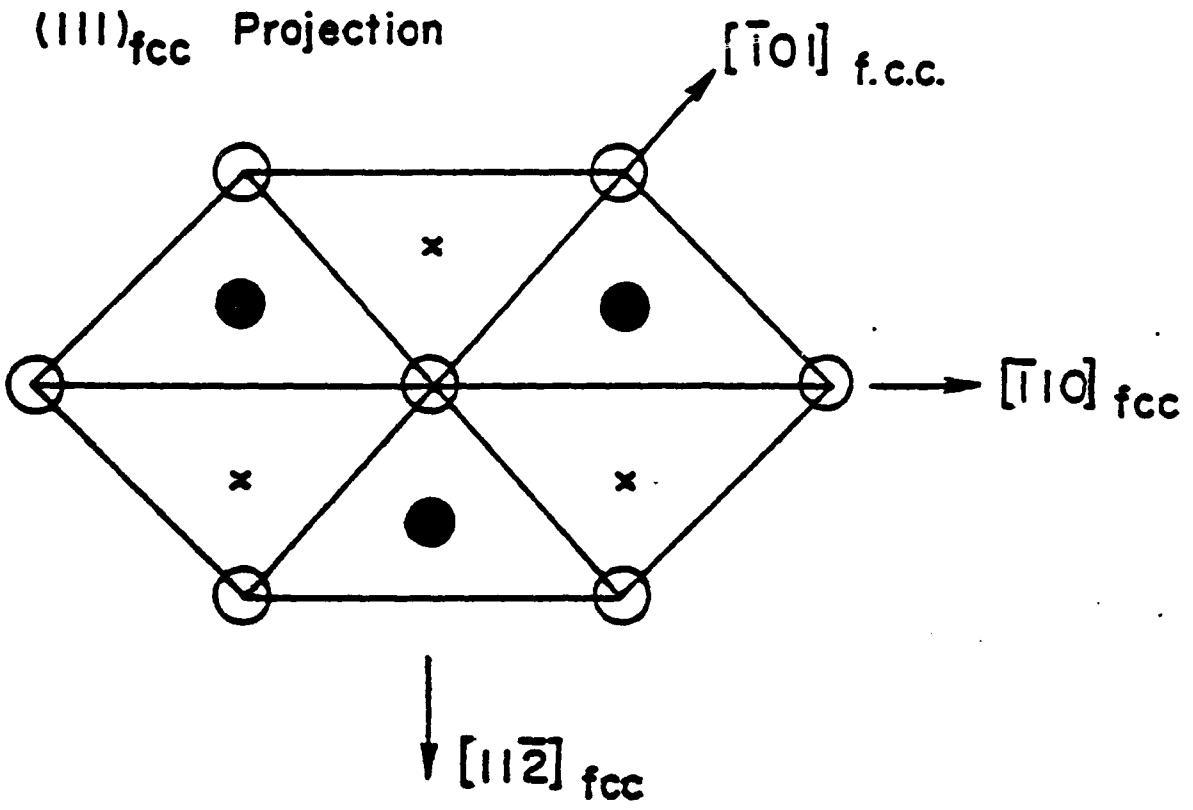

Distortions:-

In $[\,0\,1\,1\,]_\beta$ // $[\,1\,1\,1\,]_{fcc}$ $\quad \frac{a}{\sqrt{2}}\beta \rightarrow \frac{a_{fcc}}{\sqrt{3}}$

In $[\,0\,\bar{1}\,1\,]_\beta$ // $[\,1\,1\,\bar{2}\,]_{fcc}$ $\quad \sqrt{2}a_\beta \rightarrow \sqrt{\frac{6}{2}}\, a_{fcc}$

In $[\,\bar{1}\,0\,0\,]_\beta$ // $[\,\bar{1}\,1\,0\,]_{fcc}$ $\quad a_\beta \rightarrow \frac{a}{\sqrt{2}}\, fcc$

Figure 2. The (inverse) Bain correspondence between the bcc and fcc lattices and the principal lattice strain P_1 in the $(001)_{bcc}//(001)_{fcc}$ plane.

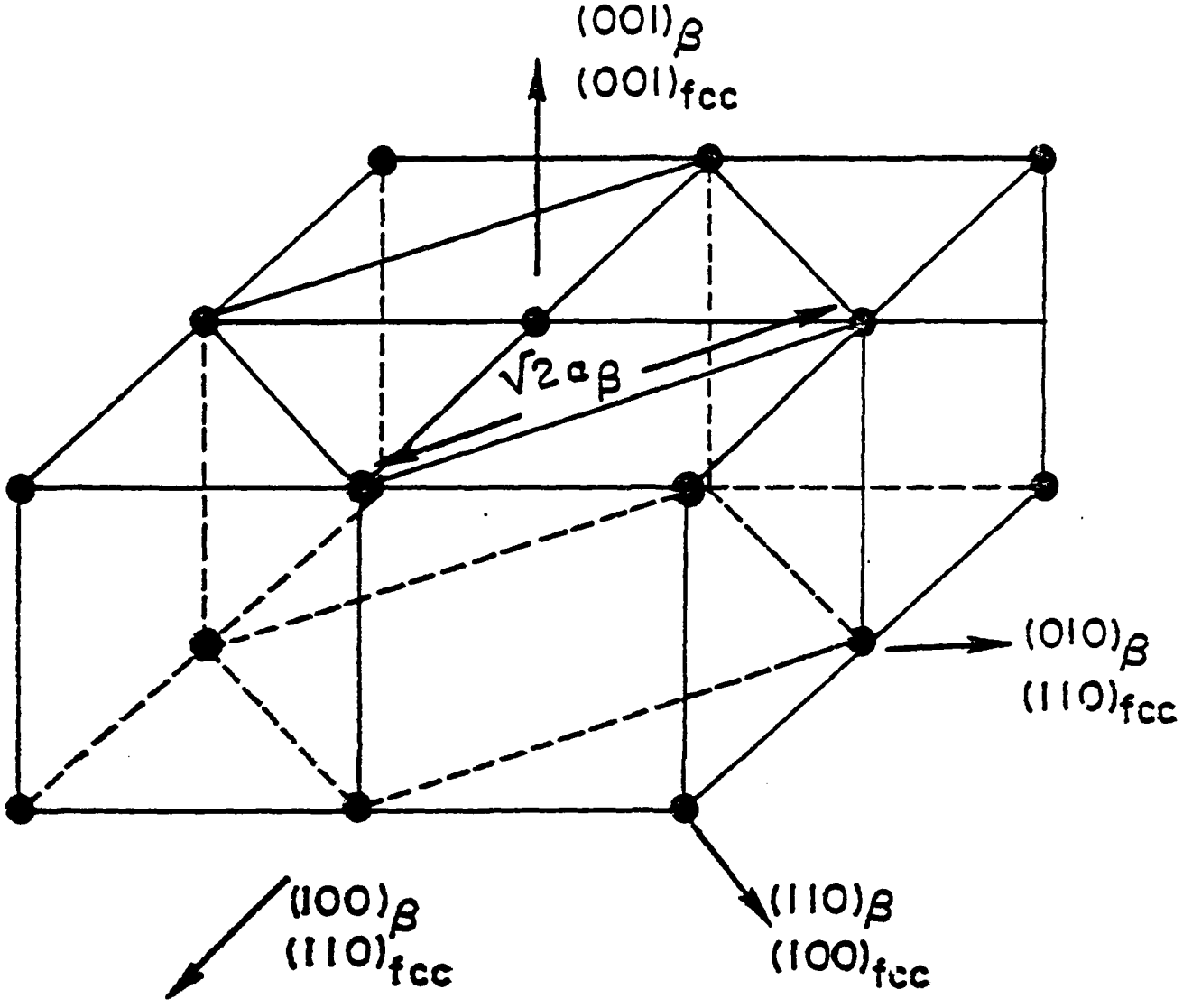

(Inverse) Bain Correspondence:

$\overline{P_1}$ = Principal Lattice Strain: $\sqrt{2}a_\beta \rightarrow \overline{a_{fcc}}$

$$P_1 = \frac{a_{fcc}}{\sqrt{2}a_\beta}$$

Figure 3. Stereogram showing the crystallography of the b.c.c f.c.c. martensite transformation for System II latt invariant shear. The arrows indicate the direction of movement of the $\{100\}_{fcc}$ poles with decreasing P values, the graduated marks on the loci indicate the positions of the $\{100\}_{fcc}$ poles for P_1 values 1.00, 0.98, 0.96, 0.94, 0.92. The locus H similarl indicates the position of the habit plane. Note that as P_1 decreases, $(111)_{fcc}$ moves towards $(011)_{b}$ and $(\bar{1}01)_{fcc}$ moves towards $(\bar{1}\bar{1}1)_{bcc}$ (shear System I: is $(011)\ [0\bar{1}1]_{bcc}$ corresponding to $(111)\ [11\bar{2}]_{fcc}$.

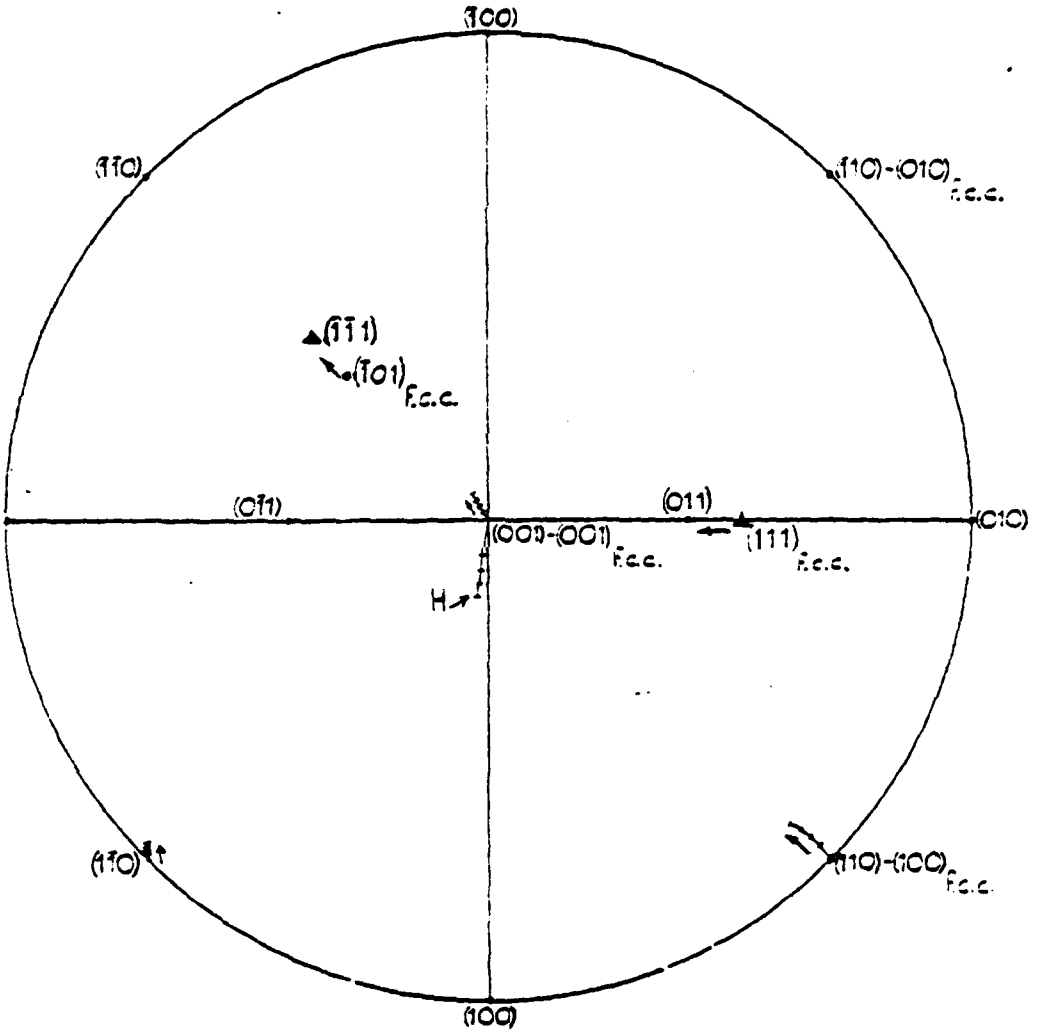
(100)
(110)-(010) F.c.c.
(111) (101) F.c.c.
(011)
(111) F.c.c.
(001)-(001) F.c.c.
H
(110)-(100) F.c.c.
(100)

Figure 4. Stereogram indicating the parallel or closely parallel shear systems in α and β for $(\bar{3}34)_\beta // (\bar{5}140$ habit plane interactions. Effect of β on initiatio of slip in α.

Abbreviations: Θ stress axes
A aids
O opposes
V very
Si significantly
St strongly

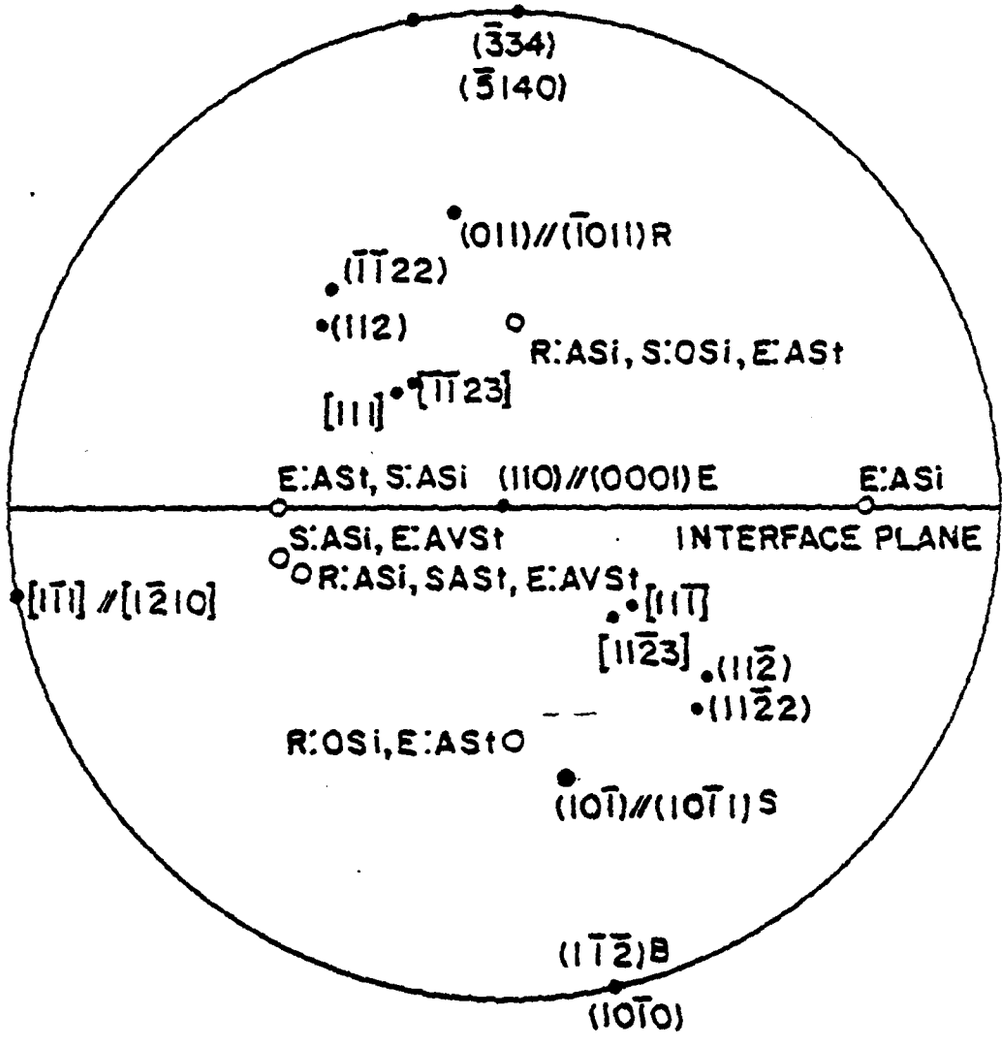
(3̄34)
(3̄140)
(011)//(1̄011)R
(1̄1̄22)
(112)
R:ASi, S:OSi, E:ASt
[111]
[11̄23]
E:ASt, S:ASi
(110)//(0001)E
E:ASi
S:ASi, E:AVSt
INTERFACE PLANE
R:ASi, SASt, E:AVSt
[1̄1̄1] //[1̄2̄10]
[111̄]
[11̄23]
(11̄2̄)
(11̄22)
R:OSi, E:ASt
(101̄)//(101̄1)S
(1̄1̄2̄)B
(101̄0)

Figure 5. Stereogram indicating parallel slip systems in α an β for $(\bar{3}34)_\beta // (\bar{1}3580)_\alpha$ habit plane.

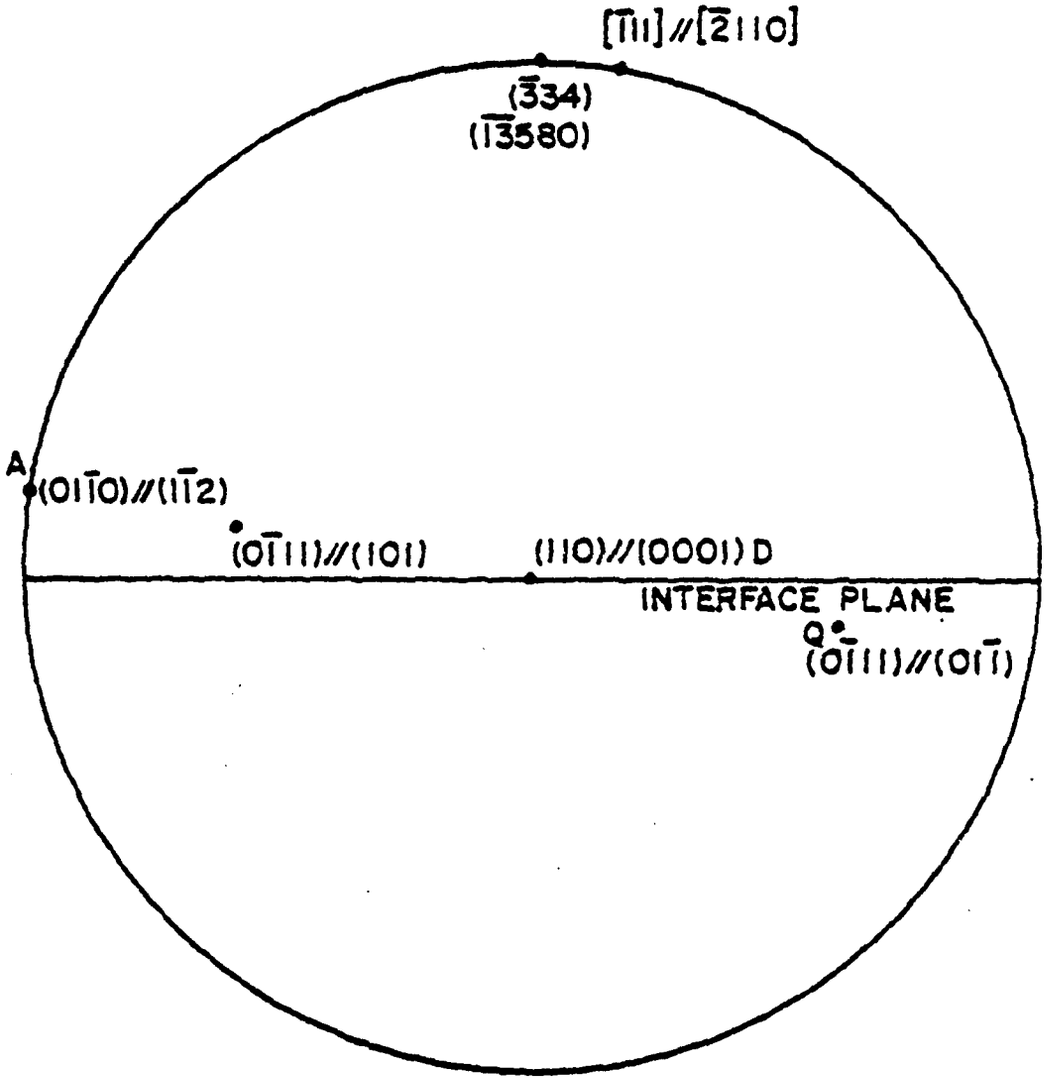
[$\bar{1}$11]//[$\bar{2}$110]
($\bar{3}$34)
($\bar{1}\bar{3}$580)
A
(01$\bar{1}$0)//(11$\bar{2}$)
(0$\bar{1}$11)//(101)
(110)//(0001) D
INTERFACE PLANE
Q
(0$\bar{1}$11)//(01$\bar{1}$)

Figure 6. Ti-1.8%Mn. Deformed 1%. Showing dislocation tangle and unidentified precipitates or inclusions

Figure 7. Ti-1.8%Mn. Deformed 1%. $\{10\bar{1}1\}_\alpha$ dark field micrograph showing dislocations in contrast.

1μ

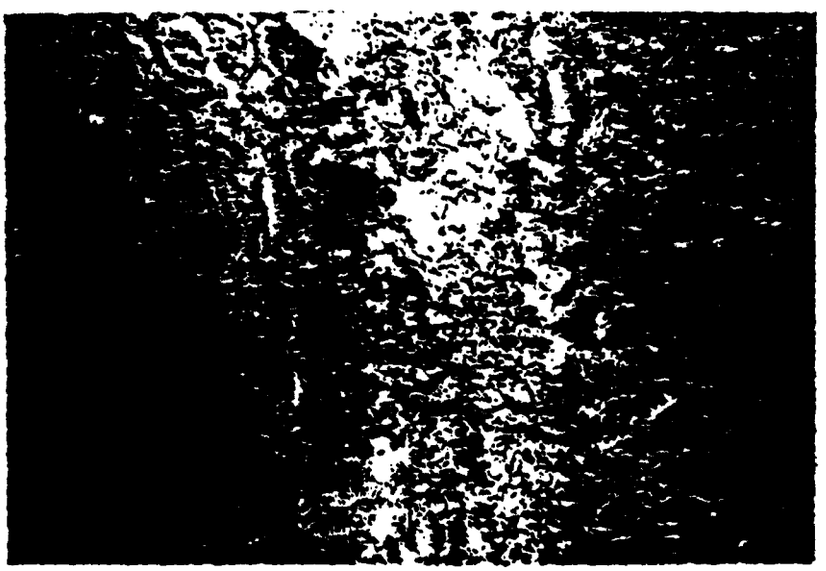

1μ

Figure 8. Ti-1.8%Mn. Deformed 1%. $(0002)_\alpha$ dark field micrograph showing Bragg contours and zero dislocation contrast. Note precipitates/inclusions in contrast.

Figure 9. Ti-1.8%Mn. Deformed 1%. Showing α (with dislocat: tangles), β and interface phase.

1μ

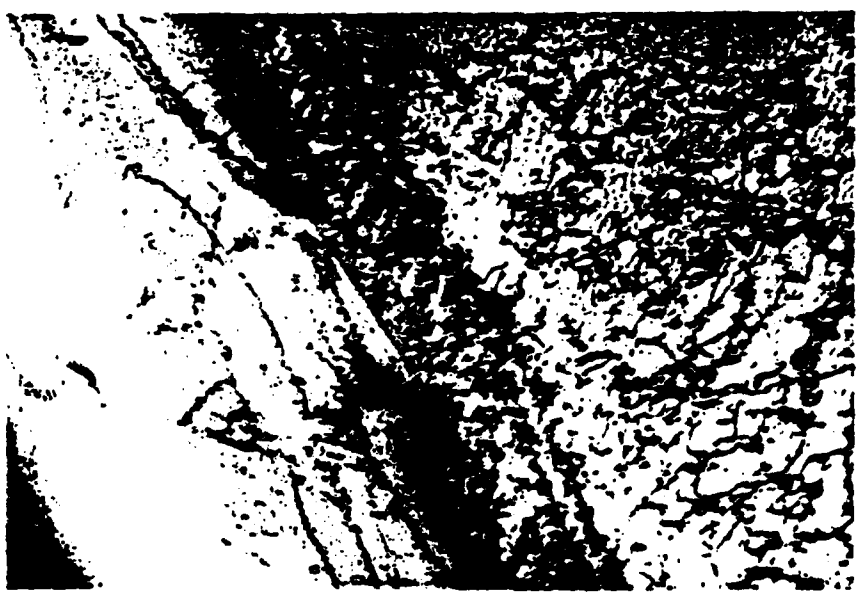

1μ

Figure 10. Ti-1.8%Mn. Deformed 1%. Dark field micrograph corresponding to Fig. 9 using $\{10\bar{1}1\}_{\alpha}$ reflection (coinciding with $\{111\}_{fcc}$ interface phase).

Figure 11. Ti-1.8%Mn. Deformed 1%. Showing α/interface phase,

1μ

1μ

Figure 12. Ti-1.8%Mn. Deformed 1%. Dark field micrograph corresponding to Fig. 11 using $\{111\}_{fcc}$ interface phase reflection.

Figure 13. Ti-1.8%Mn. Deformed 5%. Showing dislocation tangles (compare with Fig. 6).

1μ

1μ

Figure 14. Ti-1.8%Mn. Deformed 5%. Dark field micrograph using $(0002)_\alpha$ reflection, showing some $\underline{c}$ + $\underline{a}$ type dislocations in contrast.

Figure 15. Ti-1.8%Mn. Deformed 5%. Dark field micrograph of $\{21\bar{3}2\}_\alpha$ reflection showing slip bands on a $\{10\bar{1}1\}_\alpha$

1μ

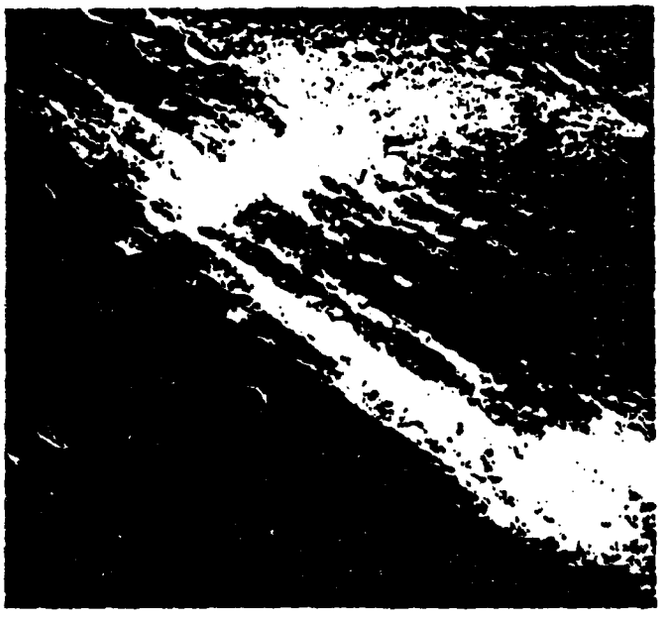

1μ

Figure 16. Ti-1.8%Mn. Deformed 5%. Dark field micrograph using common $\{110\}_\beta // \{111\}_{fcc}$ reflection showing one variant of the interface phase and a $\{112\}_\beta$ trace (A) and $\{112\}_\beta$ or $\{110\}_\beta$ traces (B & C).

Figure 17. Ti-1.8%Mn. Deformed 5%. Dark field micrograph of a $\{10\bar{1}1\}_\alpha$ reflection (c.f. Fig. 16).

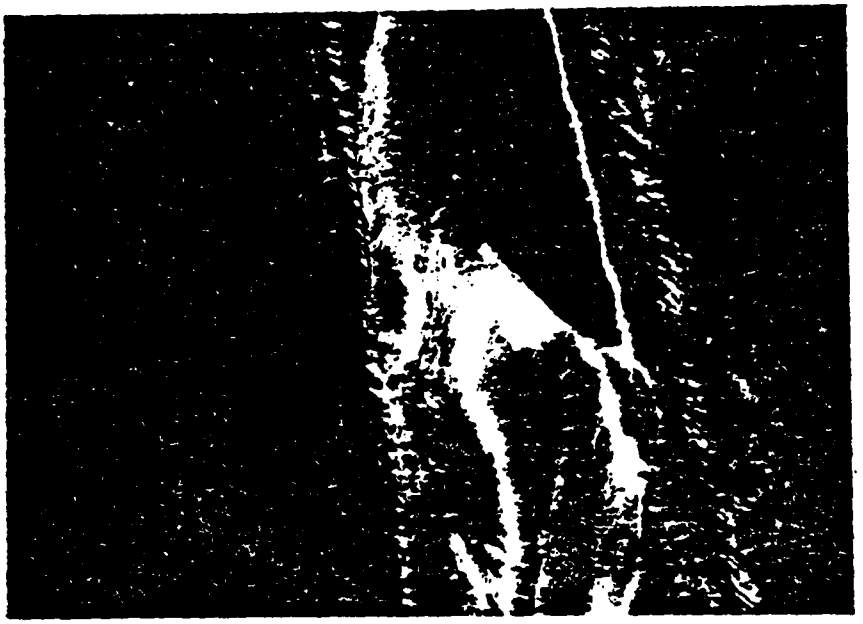

1μ

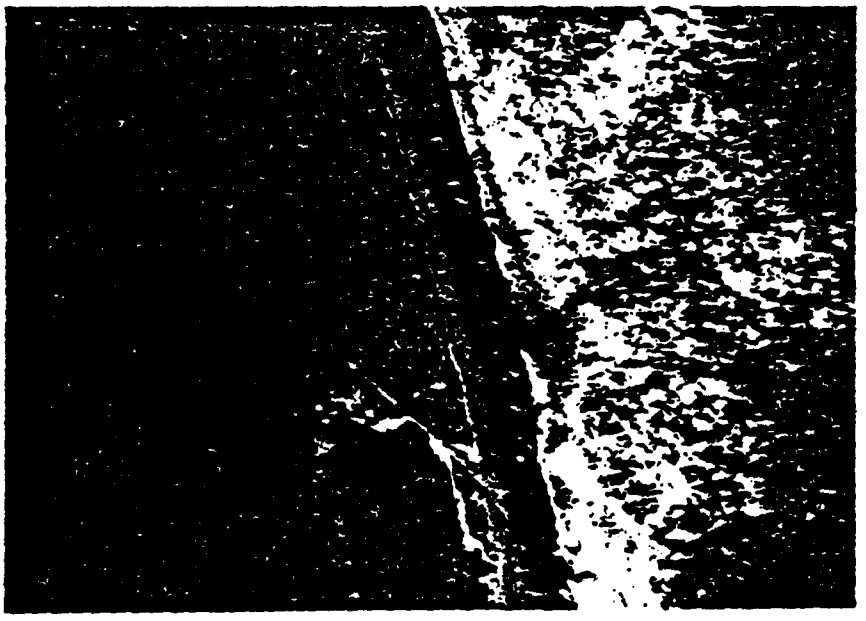

1μ

Figure 18. Ti-1.8%Mn. Deformed 6%. Dark field micrograph using a $\{11\bar{2}0\}$ reflection, showing α slip bands arrested at the interface.

Figure 19. Ti-1.8%Mn. Deformed 6%. Bright field micrograph showing slip in α and surface oxidation in the β ph

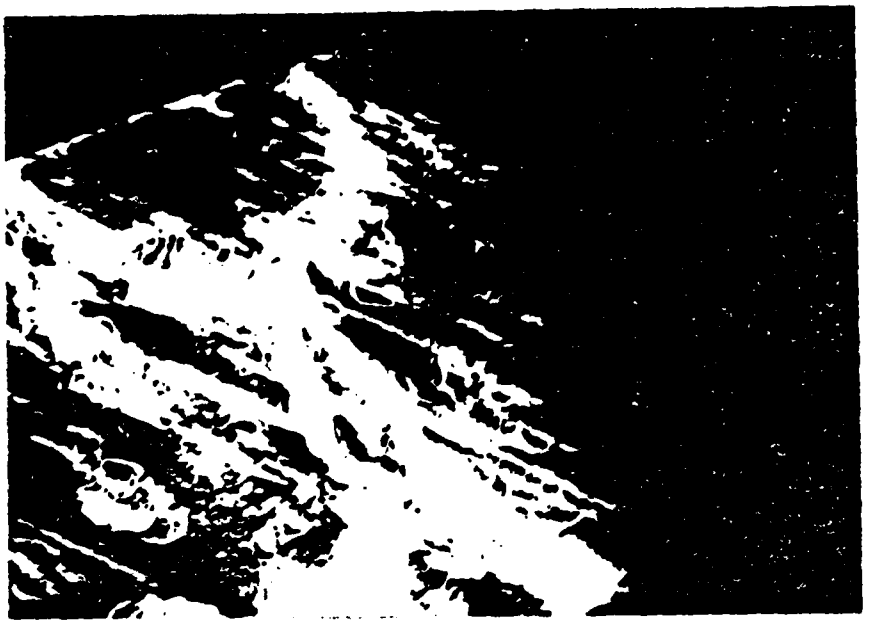

1μ

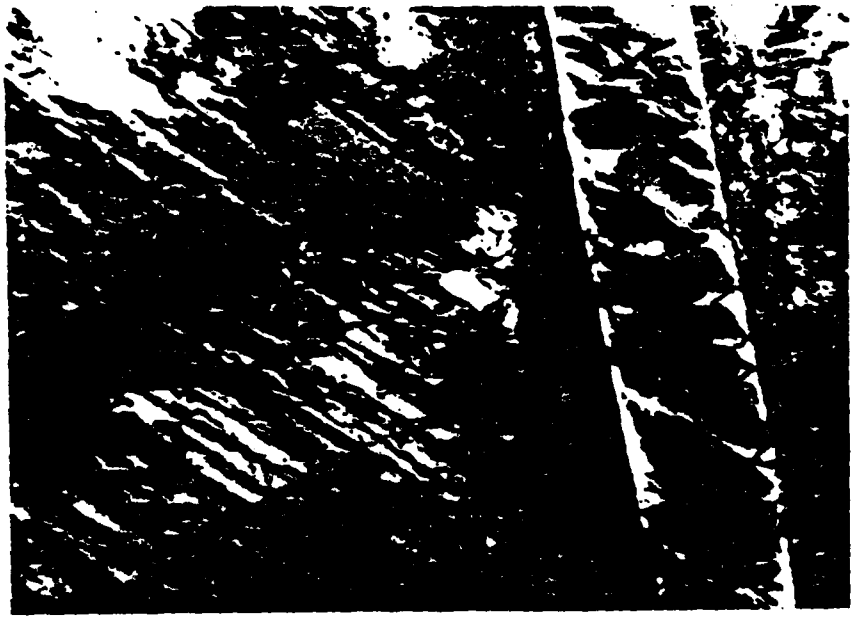

1μ

Figure 20. Ti-1.8%Mn. Deformed 6%. Bright field micrograph showing $\{10\bar{1}1\}_\alpha$ twin crossing α/β - β/α interfac

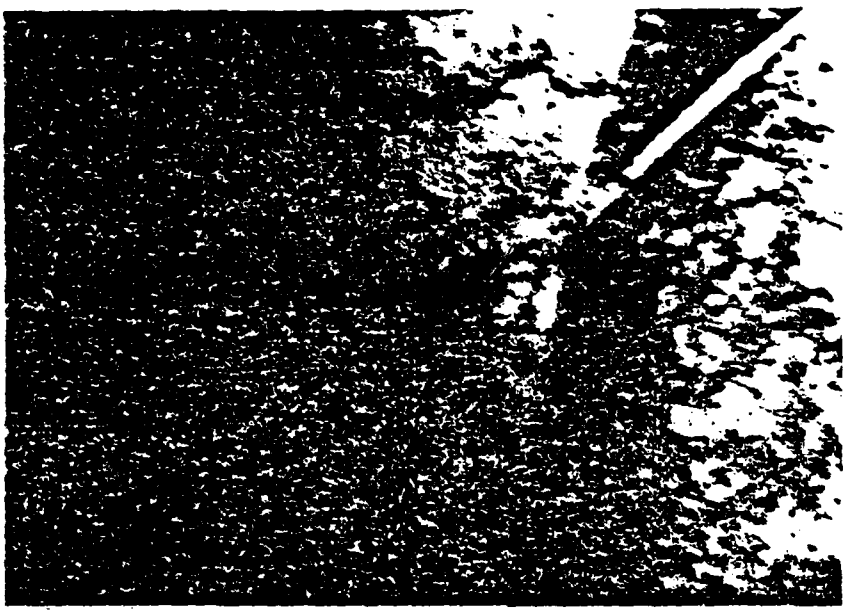

1μ

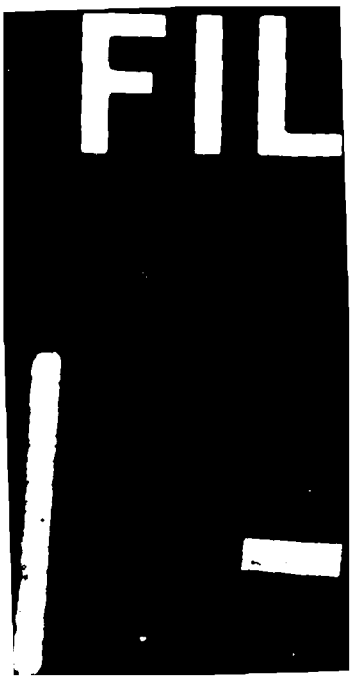
FIL